MRS Advances © 2019 Materials Research Society DOI: 10.1557/adv.2019.137



# Synthesis and characterization of Se-based nanoparticles as potential generators of reactive oxygen species

Nadja Maldonado-Luna<sup>1</sup>, Sonia Bailón-Ruiz<sup>2</sup>, Myrna Reyes-Blas<sup>3</sup>, and Oscar J. Perales-Perez<sup>4</sup>

<sup>1</sup>Department of Mechanical Engineering, University of Puerto Rico at Mayaguez

<sup>2</sup>Department of Chemistry and Physics, University of Puerto Rico at Ponce

<sup>3</sup>Department of Chemistry, University of Puerto Rico at Mayaguez

<sup>4</sup>Department of Engineering Sciences & Materials, University of Puerto Rico at Mayagüez

ABSTRACT

This work presents the synthesis of selenium-based nanoparticles via microwave-assisted heating and their subsequent characterization using UV-vis Spectroscopy (UV-Vis), highresolution transmission electron microscopy (HRTEM), and energy-dispersive X-ray spectroscopy (EDX), techniques. Ongoing research includes the study of the nanoparticles capacity to generate reactive oxygen species (ROS).

# INTRODUCTION:

The use of nanoparticles have become prominent in the biomedical field in the last few decades, giving rise to a new area that focuses on the development of nanomaterials for the prevention and treatment of different diseases [1-3]. Semiconducting nanoparticles (NPs) are promising photosensitizing materials for photodynamic therapy (PDT) applied to cancer cells due to their capability to generate cytotoxic reactive oxygen species (ROS) through a photo-stimulated chemical reaction [4-6]. There are many factors that can influence the generation of ROS by nanoparticles.

Reduced particle size increases ROS production due to the larger specific surface area permitting a greater exposure to oxygen and light absorption. The functionalization of NPs can also affect its optical properties and promote the ROS generation [7]. In particular, the potential use of metal-based NPs for PDT are based on the enhanced interaction with enzymes and proteins in mammalian cells, interfering with their antioxidant capability and leading to the generation of ROS, and subsequent apoptosis or necrosis of cells [8]. Selenium is commonly used as an anti-fungal agent [9], and as a nutritional supplement in its inorganic and organic forms based on its strong antioxidant capacity. It exists in a variety of crystalline structures, from its most stable trigonal structure to a monoclinic and less stable structure [10]. Selenium can also be found in an amorphous form, being a mix of disordered chains. The synthesis of nano-selenium can be achieved by different methods, such as chemical [11] and bacterial reduction of Se(IV) solutions [1]. On the other hand, CdSe/S Quantum dots (QDs) are also synthesized through the same microwave-assisted approach for comparison purposes. These QDs are known to generate ROS in aqueous phase [12,13].

Based on the above considerations, the present work seeks the determination of the most suitable synthesis conditions conducive to both, metallic Se and CdSe nanoparticles. Obtained results will enable their subsequent evaluation as ROS generators and their cytotoxicity against pancreatic cancer cells, PANC-1, with and without light irradiation to be published in a forthcoming manuscript.

#### **EXPERIMENTAL**

#### Synthesis of selenium nanoparticles

The synthesis of Selenium took place in a Mars6 Extraction CEM Microwave operated at 1000W. All reagents were supplied by SIGMA-ALDRICH. The synthesis was carried out in presence of ethylene glycol, the reducing agent, sodium selenite (0.0046M), sodium hydroxide (0.8M), and polyvinylpyrrolidone (0.05M) as the capping agent. All reagent solutions were added to a reaction vessel and heated in the microwave for 3-8 minutes at 180°C. A color change in the solution from colourless to a turbid orange solution, which is characteristic of selenium nanoparticles, was observed at the end of the reaction time. The resulting suspension was cooled to room temperature and formed nanocrystals were precipitated with 2-propanol, centrifuged and suspended in ethylene glycol for their characterization.

# **Synthesis of Cd-based Quantum Dots**

The protocol for the synthesis of CdSe/S is based on our previous published work [14]. Selenium (IV) and cadmium sulphate solutions were heated for 30 minutes and 190°C in a microwave digestion vessel in presence of thioglycolic acid at pH 7.0. The Cd/TGA/Se molar ratio was set at 1/4.8/0.04. The resulting translucid orange solution was cooled down to recover the nanoparticles and resuspended in deionized water

# **Characterization techniques**

The particle morphology was examined by high resolution transmission electron microscopy (HRTEM) using JEOL-2011 and JEM-ARM200F units. UV-vis absorption measurements were carried out using a Beckman DU 800 Spectrophotometer. Fourier Transform Infrared (FT-IR) Spectroscopy analysis with a LabSolutions IR

Software was also used. A Shimadtzu RF 6000 Spectrofluorometer was used to obtain the photoluminescence (PL) spectra of suspensions at room temperature.

## RESULTS AND DISCUSSION

## **Crystal structure**

Figure 1a shows a typical phase-contrast HRTEM image that evidences the crystalline structure of the selenium nanoparticles with a particle size of around 4 +- 1 nm at the end of 8 minutes. Figure 1c shows the corresponding electron diffraction pattern for the selected area; the rings in the diffraction pattern were indexed to the (110), (101) and (100) planes for selenium [15]. The two peaks at 11.2 and 12.1 keV in the EDS spectrum shown in figure 1d, correspond to selenium.

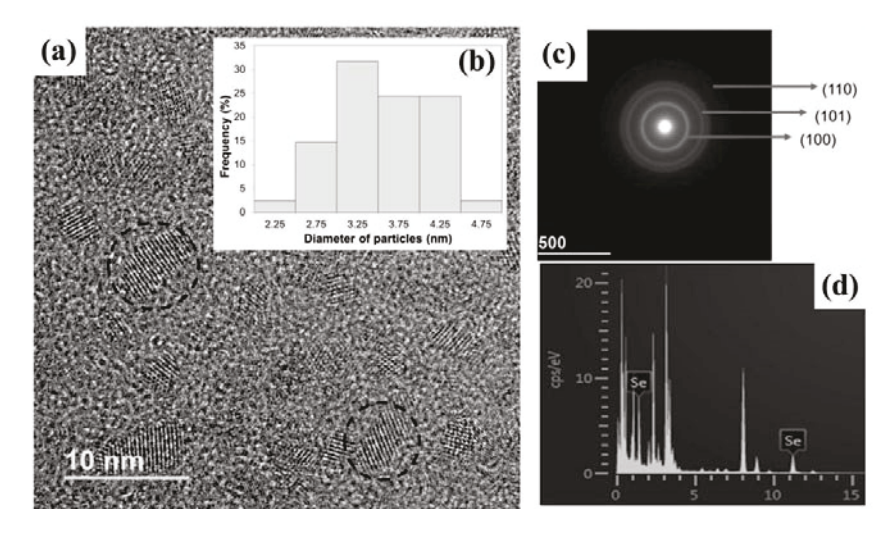


Figure 1: (a) HRTEM image, (b) Histogram of selenium nanoparticles size distribution determined from HRTEM image, (c) ED spectrum, and (d) EDS pattern of selenium nanoparticles.

Figure 2a shows the HRTEM image of as-synthesized CdSe/S QDs. The image evidenced the crystallinity of the QDs and an average particle size of 6 +- 2 nm. This results are in agreement with those obtained in our previous research [12]. Figures 2c and 2d show the electron diffraction (ED) and the energy dispersive X-Ray spectroscopy (EDS) patterns, respectively. The crystallographic planes are in accordance with the expected ones for the cubic CdSe host structure. The EDS analysis spectrum, (figure 2d), confirmed the presence of Cd and Se.

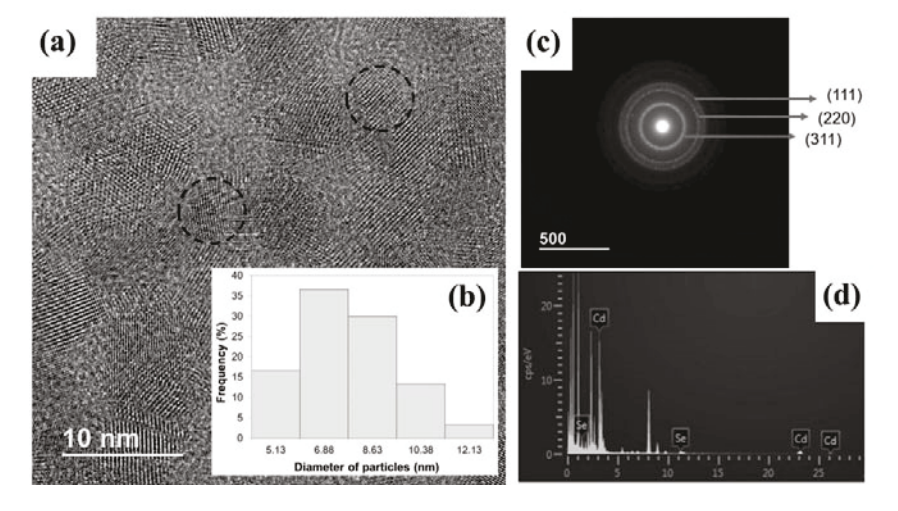


Figure 2: (a) HRTEM image, (b) Histogram of CdSe/S nanoparticles size distribution determined from HRTEM image, (c) ED spectrum, and (d) EDS pattern of TGA-CdSe/S QDs.

The FT-IR spectrum for TGA-capped CdSe/S QDs synthesized at  $190^{\circ}$  C and 30 minutes of reaction is shown in figure 3. The band at  $1566~\rm{cm^{-1}}$  is assigned to the asymmetric stretching of COO whereas the band at  $1381~\rm{cm^{-1}}$  corresponds to the symmetric stretching of COO functional group of TGA. These results confirm the presence of TGA onto CdSe/S QDs surfaces.

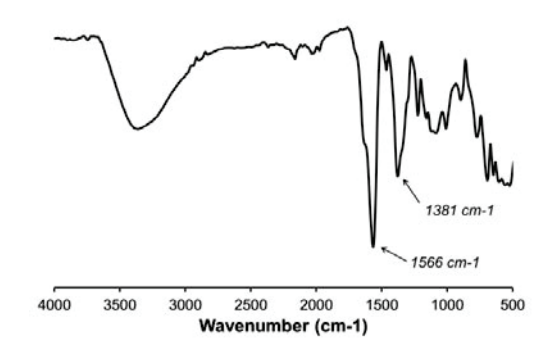


Figure 3: FT-IR spectrum for TGA-capped CdSe/S QDs synthesized at 190° C and 30 minutes of reaction.

# **Optical properties**

Figure 4 shows the UV-vis spectra for the selenium nanoparticles synthesized at 180°C for three, five and eight minutes of reaction. As evidenced, the suspension of Se nanoparticles produced at different times of reaction exhibited a strong absorption peak

centred on 260 nm. This peak is attributed to the excitation of the localized surface plasmons that causes strong light scattering by the electric field at 260 nm, where resonance occurs. The location of the peaks and their similar full width at half maximum, FWHM, values also suggest a similar crystal size for all synthesis conditions. The absorption tails and smaller peaks extending to the visible region that are observed in the UV-vis spectra can be attributed to the presence of the smaller sized particles [16]. It is characteristic of semiconducting materials such as these selenium nanoparticles to shift their absorption spectral features as a function of size.

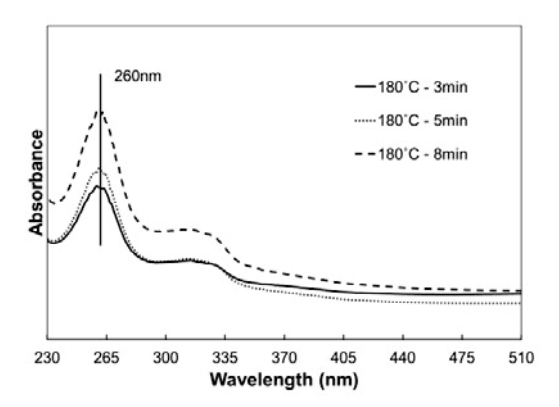
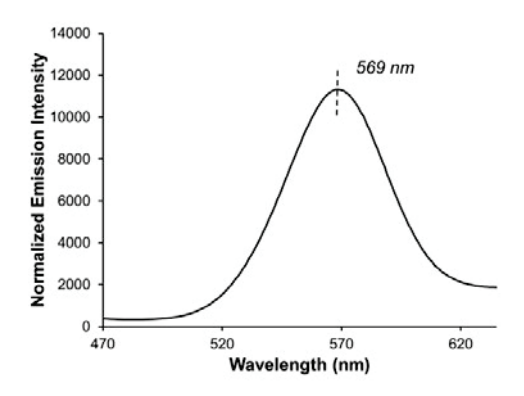


Figure 4: Absorption spectra of selenium nanoparticles synthesized at 180°C for different time intervals between three to 8 minutes.

Figure 5 depicts the photoluminescence emission° band corresponding to TGA-Capped CdSe/S QDs with a full width at half maximum  $\sim$ 52 nm, which indicates a narrow size distribution of nanocrystals. The photoluminescence peak represents the state of excitation achieved by an electron after radiative relaxation occurs, as light of sufficient energy incidences on the material.



Figure~5: Photoluminescence~spectra~for~pure~TGA-capped~CdSe/S~QDots.~The~excitation~wavelength~was~460~nm.

#### CONCLUSIONS

Se-based nanoparticles were successfully synthesized using microwave-assisted heating. For future comparison purposes, CdSe/S nanoparticles were also synthesized in aqueous phase in presence of TGA as the precursor. The obtained nanostructures were subsequently characterized through HRTEM, ED, EDS analyses that confirmed the crystal structure and composition of Se and CdSe/S nanoparticles which exhibit suitable structural properties for their evaluation as direct generators of Reactive Oxygen Species in aqueous phase.

#### **ACKNOWLEDGMENTS**

This work is supported by the Nanotechnology Center for Biomedical, Environmental and Sustainability Applications (UPRM CREST) under Grant No. HRD 0833112) and the National Institutes of Health under grant No. T34GM008419 (UPRM-MARC Program). A portion of this work was performed at the National High Magnetic Field Laboratory, which is supported by National Science Foundation Cooperative Agreement No. DMR-1644779\* and the State of Florida. We also thank the University of Puerto Rico in Ponce for its support.

### References

- P. Sonkusre and S. S. Cameotra, J. Nanobiotechnology 15, 1 (2017). [1]
- L. Kong, Q. Yuan, H. Zhu, Y. Li, Q. Guo, Q. Wang, X. Bi, and X. Gao, Biomaterials 32, 6515 [2]
- L. Shang, K. Nienhaus, and G. U. Nienhaus, J. Nanobiotechnology 12, 5 (2014). [3]
- [4] K. Ogawara and K. Higaki, Chem. Pharm. Bull. (Tokyo). 65, 637 (2017).
- J. Dong and B. Liu, Chemotherapy 05, (2016). [5]
- [6] M. H. Raza, S. Siraj, A. Arshad, U. Waheed, F. Aldakheel, S. Alduraywish, and M. Arshad, J. Cancer Res. Clin. Oncol. 143, 1789 (2017).
- [7] J. Zhao, Y. Li, E. Shang, and W. Pang, Glob. J. Nanomedicine 1, 10 (2017).
- J. Sun, S. Kormakov, Y. Liu, Y. Huang, D. Wu, and Z. Yang, Molecules 23, 1704 (2018). [8]
- [9] Q. Wang, A. Mejía Jaramillo, J. J. Pavon, and T. J. Webster, J. Biomed. Mater. Res. - Part B Appl. Biomater. 104, 1352 (2016).
- [10] P. Cherin and P. Unger, Inorg. Chem. 6, 1589 (1967).
- [11] S. Y. Zhang, J. Zhang, H. Y. Wang, and H. Y. Chen, Mater. Lett. 58, 2590 (2004).
- [12] E. Calderón-Ortiz, S. Bailón-Ruiz, L. Alamo-Nole, J. Rodriguez-Orengo, and O. Perales-Perez, MRS Proc. 1784, mrss15 (2015).
- [13] S. Bailón-Ruiz and O. J. Perales-Pérez, Appl. Mater. Today 9, 161 (2017).
- [14] S. Bailon-Ruiz, L. Alamo-Nole, and O. Perales-Perez, Curr. Nanosci. 8, 202 (2012).
- [15] C. P. Shah, K. K. Singh, M. Kumar, and P. N. Bajaj, Mater. Res. Bull. 45, 56 (2010).
- Z. Lin and C. R. C. Wang, Mater. Chem. Phys. 92, 591 (2005).